JOURNAL OF VIROLOGY, Feb. 2009, p. 1402–1415 Vol. 83, No. 3
0022-538X/09/$08.00+0 doi:10.1128/JVI.01138-08

SOCS-1 Mimetics Protect Mice against Lethal Poxvirus Infection: Identification of a Novel Endogenous Antiviral System▽

Chulbul M. Ahmed,†* Rea Dabelic,† Lilian W. Waiboci, Lindsey D. Jager, Linda L. Heron, and Howard M. Johnson

Department of Microbiology and Cell Science, University of Florida, P.O. Box 110700, Gainesville, Florida 32611-0700

Received 30 May 2008/Accepted 7 November 2008

The suppressor of cytokine signaling 1 (SOCS-1) protein modulates cytokine signaling by binding to and inhibiting the function of Janus kinases (JAKs), ErbB, and other tyrosine kinases. We have developed a small tyrosine kinase inhibitor peptide (Tkip) that binds to the autophosphorylation site of tyrosine kinases and inhibits activation of STAT transcription factors. We have also shown that a peptide corresponding to the kinase-inhibitory region of SOCS-1, SOCS1-KIR, similarly interacts with the activation loop of JAK2 and blocks STAT activation. Poxviruses activate cellular tyrosine kinases, such as ErbB-1 and JAK2, in the infection of cells. We used the pathogenesis of vaccinia virus in C57BL/6 mice to determine the ability of the SOCS-1 mimetics to protect mice against lethal vaccinia virus infection. Injection of mice intraperitoneally with Tkip or SOCS1-KIR containing a palmitate for cell penetration, before and at the time of intranasal challenge with 2×10^6 PFU of vaccinia virus, resulted in complete protection at 100 μg. Initiation of treatment 1 day postinfection resulted in 80% survival. Administration of SOCS-1 mimetics by the oral route also protected mice against lethal effects of the virus. Both SOCS1-KIR and Tkip inhibited vaccinia virus transcription and replication at early and possibly later stages of infection. Vaccinia virus-induced phosphorylation of ErbB-1 and JAK2 was inhibited by the mimetics. Protected mice mounted a strong humoral and cellular response to vaccinia virus. The use of SOCS-1 mimetics in the treatment of poxvirus infections reveals an endogenous regulatory system that previously was not known to have an antiviral function.

Poxviruses are complex, large, double-stranded DNA viruses that replicate in the cytoplasm of the cell. The variola strain of poxviruses is responsible for some of the most devastating pandemics in the history of mankind and is estimated to have caused up to 500 million smallpox deaths worldwide in the 20th century (16, 22). Remarkably, global immunization has essentially eradicated smallpox, but with discontinuation of vaccination for more than several decades, the world population is highly vulnerable to reintroduction of the virus either accidentally or deliberately.

Poxviruses are highly adept at evading host innate defense mechanisms because of the many poxvirus evasion genes (7, 23). There are, for example, greater than 18 proteins that are produced by poxviruses that interfere with a variety of host defense factors. The interferon (IFN) system is particularly ineffectual in inhibiting poxviruses such as vaccinia virus, where both type I and type II IFNs are inactivated by virus-induced decoy receptors (7, 23).

We have circumvented the neutralizing effects of vaccinia virus IFN-γ decoy receptor B8R by the development of a small-peptide mimetic of IFN-γ that functions intracellularly (1–3). The only antiviral drug that has been approved for the treatment or prevention of poxvirus infections is an acyclic nucleoside phosphonate called cidofovir (6, 12, 16, 27, 29). Cidofovir is not effective orally and may cause renal toxicity. Thus, there is much interest in other therapeutics. Recently, it was shown that inhibitors of key cellular tyrosine kinases could reduce the virulence and lethality of poxvirus infection (28, 35), which suggests a novel approach to thwarting the pathogenicity of these viruses. Specifically, the Abl tyrosine kinase inhibitor Gleevec protected mice against lethal vaccinia virus infection (28), while the epidermal growth factor (EGF) receptor ErbB-1 inhibitor CI-1033 similarly protected mice against vaccinia virus (35). Neither kinase inhibitor interfered with vaccinia virus replication, but Gleevec inhibited the release of extracellular enveloped virus (EEV) from actin tails (28). Vaccinia virus and variola virus code for EGF-related growth factors called vaccinia virus growth factor (VGF) and smallpox virus growth factor (SPGF), respectively (9, 17). These growth factors act on ErbB-1 and are important for virus replication and release (9, 10, 26, 32). In this regard, the kinase inhibitors, through their action on ErbB-1, may block downstream effects of ErbB-1 by inactivating other kinases such as Src. A different kind of drug called ST-246 has recently been shown to have therapeutic effects against vaccinia virus infections in mice (34). ST-246 was discovered by high-throughput screening of thousands of compounds. Among the drugs mentioned here, the IFN mimetic is unique in that it is directly related to the endogenous IFN antiviral pathway of the host defense (1–3).

We have developed small-peptide mimetics of the negative cytokine regulatory protein suppressor of cytokine signaling 1 or SOCS-1, which is another approach to the development of a novel endogenous antiviral pathway (13, 14, 33). These tyrosine kinase inhibitor peptides, similar to SOCS-1, inhibit the Janus kinase JAK2, as well as ErbB-1. One mimetic corre-

* Corresponding author. Mailing address: Department of Microbiology and Cell Science, University of Florida, P.O. Box 110700, Gainesville, FL 32611-0700. Phone: (352) 392-6883. Fax: (352) 392-5922. E-mail: ahmed1@ufl.edu.

† These authors contributed equally to this work.

▽ Published ahead of print on 19 November 2008.

TABLE 1. Amino acid sequences of the peptides used in this study and alignment with SOCS5-KIR[a]

Peptide	Sequence
SOCS1-KIR	^{53}DTHFRTFRSHSDYRRI
SOCS1-KIR2A	^{53}DTHFATFASHSDYRRI
SOCS5-KIR	**W**K**V**H-TQ**I**D**Y**
Tkip	**W**L**V**F-FV**I**F**Y**FFR
Tkip2A	WLVFFVIAYFAR
Tkip5A	WLVAAVIAYFAA
IFN-γ(95-106)	^{95}AKFEVNNPQVQR
IFN-γ(95-132)	^{95}AKFEVNNPQVQRQAFNELIRVVHQLLPESSLR KRKRSR

[a] All of the peptides were synthesized with an attached lipophilic group, palmitic acid, for cell penetration. SOCS1-KIR2A and Tkip2A are alanine substitution-containing mutant forms of SOCS1-KIR and Tkip, respectively, that do not show any biological activity. IFN-γ(95-106) is a truncated form of IFN-γ(95-132) and lacks any biological activity. The SOCS5-KIR sequence is presented for comparison with the Tkip sequence. Identical residues in SOCS5-KIR and Tkip, as described by Nicholson and colleagues (11), are in boldface type.

sponds to the kinase-inhibitory region (KIR) of SOCS-1 and is referred to as SOCS1-KIR (36). The other was developed based on hydropathic complementarity to the autophosphorylation site of JAK2 and is referred to as the tyrosine kinase-inhibitory peptide or Tkip (13, 14). We thus examined whether SOCS1-KIR and Tkip could inhibit vaccinia virus replication in cell culture, as well as blockage of lethal vaccinia virus infection of mice. JAK2 is of particular interest, since tyrophostin AG490, an inhibitor of JAK2 and other kinases, has been shown to inhibit myxoma virus replication (21). Our data show that SOCS1-KIR and Tkip are effective inhibitors of lethal vaccinia virus infection. Additionally, unlike Gleevec and CI-1033, these JAK inhibitors blocked the production of infectious vaccinia virus particles and not simply the release of EEV. Thus, the SOCS-1 mimetics may represent potent therapeutics against poxviruses. Recently, it has been suggested that the host response to poxvirus infection may contribute to virus pathology via overproduction of cytokines, resulting in a "cytokine storm," which ends up causing more harm than the virus itself (16, 30). Negative regulators of cytokines, such as SOCS1-KIR and Tkip, may have a role in suppressing this cytokine storm via inhibition of kinases such as JAK2.

MATERIALS AND METHODS

Cells and virus. BSC-40, L929, and WISH cells were obtained from the American Type Culture Collection (Manassas, VA) and propagated on Dulbecco modified Eagle medium with 10% fetal bovine serum. All cells were grown at 37°C in a humidified atmosphere with 5% CO_2. The vaccinia virus Western Reserve strain was a kind gift from Richard Condit (University of Florida). Vaccinia virus was grown, titrated on BSC-40 cells, and purified on a sucrose gradient as described previously (5).

Peptides. The sequences of the peptides used in this study are presented in Table 1. These peptides were synthesized on an Applied Biosystems 9050 automated peptide synthesizer by conventional 9-fluorenylmethoxy carbonyl chemistry as described previously (31). The addition of a lipophilic group (palmitoyllysine) to the N terminus of the synthetic peptide was performed as a last step by a semiautomated protocol. Peptides were characterized by mass spectrometry and purified by high-pressure liquid chromatography.

Binding assays. Binding assays were performed as previously described (13), with minor modifications. Tkip, Tkip2A, SOCS1-KIR, SOCS1-KIR2A, and a control peptide were bound to 96-well plates in binding buffer (0.1 M sodium carbonate-sodium bicarbonate [pH 9.6]) at 3 μg/well. The wells were washed three times in wash buffer (0.05% Tween 20 in Tris-buffered saline) and incubated in blocking buffer (2% gelatin and 0.05% Tween 20 in phosphate-buffered saline [PBS]) for 1 h at room temperature. Wells were then washed three times and incubated with various concentrations of biotinylated JAK2(1001-1013) for 1 h at room temperature. Following incubation, wells were washed five times and bound biotinylated peptides were detected with horseradish peroxidase (HRP)-conjugated neutravidin (Molecular Probes, Eugene, OR) and *o*-phenylenediamine (OPD) in stable peroxidase buffer (Pierce, Rockford, IL). The chromogenic reaction was stopped by the addition of 2 M H_2SO_4 (50 μl) to each well. Absorbance was measured at 490 nm with a 450 microplate reader (Bio-Tek, Winooski, VT). Similar binding assays were performed with an antibody enzyme-linked immunosorbent assay (ELISA). Briefly, peptides were bound as described above; this was followed by washing and blocking for 1 h. Wells were then washed three times and incubated with various concentrations of SOCS1-KIR for 1 h at room temperature. Following incubation, wells were washed five times, serum obtained from rabbits immunized with SOCS1-KIR peptide conjugated to keyhole limpet hemocyanin (GenScript Corporation, Piscataway, NJ) was added, and the mixture was incubated for 1 h at room temperature. Wells were washed five times and incubated with a goat anti-rabbit immunoglobulin G (IgG)-HRP conjugate (Santa Cruz Biotechnology, Santa Cruz, CA); this was followed by washing and addition of OPD. The chromogenic reaction was stopped by the addition of 2 M H_2SO_4 (50 μl) to each well. Absorbance was measured at 490 nm with a 450 microplate reader.

Western blot analysis. Western blot analysis was carried out to determine whether Tkip and SOCS1-KIR inhibited the phosphorylation of the STAT substrate by the various JAKs in cultured cells. Cells were incubated with various concentrations of lipophilic Tkip, Tkip2A, SOCS1-KIR, SOCS1-KIR2A, or a control peptide for 2 h, after which IFN was added and the cells were incubated for an additional 2 h. The cells were washed in cold PBS and harvested in radioimmunoprecipitation assay buffer containing protease and phosphatase inhibitor cocktails (Santa Cruz). Protein concentration was measured with a bicinchoninic acid assay kit (Pierce), and lysates were resolved by 12% sodium dodecyl sulfate-polyacrylamide gel electrophoresis (SDS-PAGE), transferred onto nitrocellulose membranes, and probed with various antiphosphotyrosine antibodies. The membranes were then stripped and reprobed with the indicated antiprotein antibodies. All of the antibodies used were from Santa Cruz Biotechnology. Scanning of band intensity was carried out with Image J software from NIH.

Mice. All of the animal protocols used were approved by the Institutional Animal Use and Care Committee at the University of Florida. Female C57BL/6 mice (6 to 8 weeks old) were purchased from Jackson Laboratories (Bar Harbor, ME). Peptides dissolved in PBS in a volume of 100 μl were administered intraperitoneally (i.p.). For oral administration of the peptides, the indicated amounts of peptide in 0.5 ml PBS were given with a feeding needle. I.p. administration of vaccinia virus was done in a volume of 100 μl. For intranasal administration, vaccinia virus was taken in a volume of 10 μl, and 5 μl was delivered into each of the nostrils of a lightly anesthetized mouse. Following infection, mice were observed daily for signs of disease such as lethargy, ruffled hair, weight loss, and eye secretions. Moribund mice were euthanized and counted as dead.

Measurement of intracellular and extracellular vaccinia virus formation. BSC-40 cells were seeded and grown overnight to confluence. Peptides at the concentrations indicated were added to cells, which were incubated for 1 h and then infected with vaccinia virus at a multiplicity of infection (MOI) of 5 for 1 h. This was followed by addition of growth medium containing the same amount of peptides as before and incubation for the time periods indicated. Supernatants were harvested, and the cells were scraped into 0.2 ml of cell lysis buffer consisting of 50 mM Tris-HCl (pH 7.5), 250 mM NaCl, 0.1% NP-40, 50 mM NaF, and 5 mM EDTA and then subjected to three cycles of freeze-thawing and sonication. The virus titers in the supernatants (extracellular) and cell extracts (intracellular) were measured by plaque assay on BSC-40 cells.

Measurement of vaccinia virus-specific cellular response by proliferation assay. Spleens obtained from naïve mice or mice that recovered at the times indicated were homogenized to a single-cell suspension. Splenocytes (10^5 cells per well) were incubated with medium alone or medium containing UV-inactivated vaccinia virus at 37°C for 96 h. The cultures were then pulsed with [^{3}H]thymidine (1 μCi/well; Amersham Biosciences) for 8 h before harvesting onto filter paper discs with a cell harvester. Cell-associated radioactivity was counted with a scintillation counter.

Measurement of vaccinia virus-specific cellular response by IFN-γ ELISPOT assay. CD4 depletion of splenocytes from naïve mice or mice that recovered was carried out with the L3T4 antibody bound to Dynabeads (Invitrogen, Carlsbad, CA). An enzyme-linked immunospot (ELISPOT) assay was carried out with a kit from Mabtech USA. Briefly, CD4-depleted cells (10^5 per well) were seeded into a microtiter plate that had previously been coated with an antibody to IFN-γ and incubated in the absence or presence of increasing amounts of purified vaccinia virus for 24 h at 37°C. After washing, diluted monoclonal antibody was added,

the mixture was incubated for 2 h and washed, and streptavidin-HRP was added. After 1 h at room temperature, the wells were washed, 3,3′5,5′-tetramethylbenzidine substrate was added, and absorbance was measured in a plate reader.

Measurement of anti-vaccinia virus antibody response by ELISA. Microtiter plates were coated with 10^6 PFU of purified, UV-inactivated (900,000 $\mu J/cm^2$ for 5 min in a DNA cross-linker) vaccinia virus in 100 μl of binding buffer (carbonate-bicarbonate [pH 9.6]) overnight at 4°C. Plates were blocked for 2 h at room temperature with PBS containing 5% fetal bovine serum. Mouse serum was serially diluted in PBS containing 0.1% Tween 20 (wash buffer). A 0.1-ml volume of the diluted serum was added to each well. The plate was incubated for 2 h at room temperature and washed three times with wash buffer. Peroxidase-conjugated goat anti-mouse IgA (α chain specific) or IgG (γ chain specific) (both from Santa Cruz Biotechnology, Santa Cruz, CA), diluted in a volume of 0.1 ml, was added to each well, and the plates were incubated for 1 h and washed five times with wash buffer. OPD in a volume of 0.1 ml was added, and the mixture was incubated for 15 min. The reaction was stopped by the addition of 50 μl of 3 N HCl. The optical density at 490 nm was determined with a microtiter plate reader.

Measurement of vaccinia virus-neutralizing antibodies. A plaque reduction assay was carried out to test the ability of antibodies to inhibit viral infection of target cells, by the procedure previously described (15). BSC-40 cells were seeded to confluence in a six-well plate the day before the assay. Sera obtained from mice on the days indicated were heated at 56°C for 30 min to inactivate the complement. Purified vaccinia virus (100 PFU) was incubated with a known dilution of serum at 37°C for 1 h and then added to BSC-40 cells. One hour later, the virus-containing medium was replaced with fresh medium containing 0.5% agarose and 0.01% neutral red. Three days later, the plaques were counted. The number of plaques in wells with vaccinia virus alone was taken as 100%. The percent reduction in other treatments carried out in triplicate was measured and is presented as the average and standard deviation.

Western blot analysis for JAK2 and EGFR. For the Western blot assays shown below (see Fig. 9), cells were treated with 25 μM SOCS-1 mimetic or a control peptide for 1 h and then infected with vaccinia virus (MOI of 5) for the times indicated. Cells were washed in PBS and harvested in radioimmunoprecipitation assay buffer containing protease inhibitor cocktail (Santa Cruz Biotechnology, Santa Cruz, CA). Protein concentration was measured with a bicinchoninic acid assay kit from Pierce (Rockford, IL). Protein (50 μg of each) was immunoprecipitated with phosphotyrosine antibody, electrophoresed on an acrylamide gel, transferred to an Immobilon-P filter, and probed with the antibodies indicated. HRP-conjugated antibodies were used. Detection was by chemiluminescence (Pierce). All of the antibodies used were from Santa Cruz Biotechnology. Scanning of band intensity was carried out with Image J software from NIH.

Quantitative RT-PCR. BSC-40 cells were treated with Tkip, SOCS1-KIR, or a control peptide or mock treated for 1 h and then infected with vaccinia virus (MOI of 5) for 1 h. The virus was washed away, and the cells were incubated for 18 h in the presence of peptides. Total RNA was extracted with Trizol reagent (Invitrogen, Carlsbad, CA) and treated with DNase (Invitrogen, Carlsbad, CA) to remove contaminating DNA. One microgram of total RNA was used to synthesize the first strand of cDNA with the random hexamer and the reagents provided in a reverse transcriptase kit from Bio-Rad (Hercules, CA). The cDNA was diluted 1:100, and 1 μl of the diluted cDNA was taken in a 50-μl reaction mixture with primers and a PCR mixture containing SYBR green (Bio-Rad, Hercules, CA) and used for PCR in a Mini Opticon thermal cycler (Bio-Rad, Hercules, CA). The following conditions were used. Initial denaturation was carried out at 94°C for 5 min and followed by 45 cycles of denaturation at 94°C for 30 s, annealing at 55°C for 30 s, and polymerization at 72°C for 30 s. This was followed by incubation at 72°C for 7 min. The following primers were used. Early transcription was followed with primers from the D12L gene (forward primer 5′-GAACGCATGTCCTTCTTCCA-3′ and reverse primer 5′-CATGTCGGT CGGCATTCTAT-3′). The A1L gene was used for intermediate gene transcription (forward primer 5′-GGGTGGTGAAGTTGGGTATT-3′ and reverse primer 5′-CTTCCGTAAACGCCGTCTTT-3′). For late gene transcription, A7L primers were used (forward primer 5′-CGCGTCCGATATAGGAAAGA-3′ and reverse primer 5′-CATTCCCGCGTCAGATTGAA-3′). For actin transcription, forward primer 5′-GGACTTCGAGCAAGAGATGG-3′ and reverse primer 5′-AGCACTGTGTTGGCGTACAG-3′ were used. The expression of early, intermediate, and late genes was normalized to the levels of actin gene expression, and the relative levels of different transcripts were analyzed with the Genex software from Bio-Rad (Hercules, CA).

Statistical analysis. All experimental data on mouse studies were measured for statistical significance by the Kaplan-Meier survival curve and the log rank test with the GraphPad Prism software from GraphPad Software, Inc., San Diego, CA.

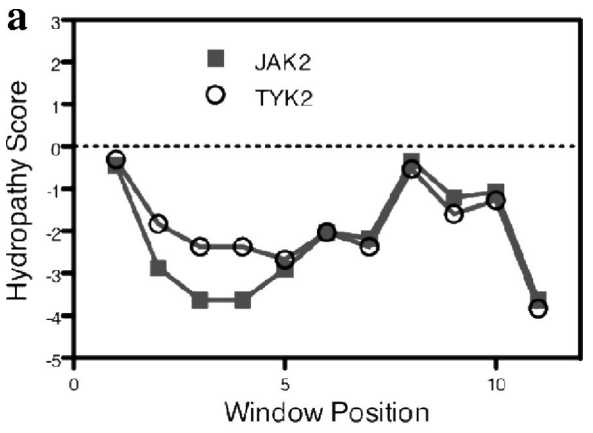

FIG. 1. Hydropathic profiles of the JAK kinase JAK2 and TYK2 autophosphorylation sites and sequence alignment. (a) Hydropathic profiles of murine JAK2 and TYK2 as determined by the Kyte-Doolittle hydropathic plot (18) with a window of three amino acids. The two JAKs have similar, but not identical, profiles, suggesting similar structures. (b) Alignment of the amino acid sequences of the autophosphorylation sites of murine JAK kinases JAK2 and TYK2.

RESULTS

SOCS1-KIR and Tkip recognition of autophosphorylation sites of different JAKs with biotinylated peptides. SOCS-1 has been reported to recognize and modulate the function of the JAKs (4, 11, 36, 37). We were interested, therefore, in determining the ability of SOCS1-KIR and Tkip to bind to and modulate the kinase activity of JAK2 and TYK2, as these JAKs are involved in type I and type II IFN signaling. First, we plotted the hydropathic profiles of the JAK autophosphorylation sites with the Kyte-Doolittle hydropathic plot (18). The two JAKs have similar, but not identical, profiles, suggesting similar structures (Fig. 1a). In general, the amino acid sequences of the autophosphorylation sites of the JAKs show significant homology (Fig. 1b).

We have previously shown that Tkip and SOCS1-KIR bound to the autophosphorylation or activation loop site of JAK2 (33). We therefore synthesized peptides corresponding to the autophosphorylation sites of the JAKs (Fig. 1b) and compared TYK2 with JAK2 for binding to SOCS1-KIR and Tkip. As previously reported, SOCS1-KIR and Tkip bound to the JAK2 autophosphorylation site (Fig. 2a) (33). SOCS1-KIR and Tkip also specifically bound to the autophosphorylation site of TYK2 (Fig. 2b), a JAK that plays a key role in the mediation of type I IFN signaling (20). Thus, SOCS1-KIR and Tkip bind to the autophosphorylation sites of the IFN JAK kinases. Further, the KIR of SOCS-1 may be key to SOCS-1 recognition of the JAKs.

Phenylalanines at positions 56 and 59 of SOCS-1 have previously been identified as critical for SOCS-1 binding to JAK2 and for its function (36). Accordingly, the bindings in Fig. 2 also include SOCS1-KIR with alanine substitutions at positions 56 and 59 (SOCS1-KIR2A), as well as Tkip with alanine sub-

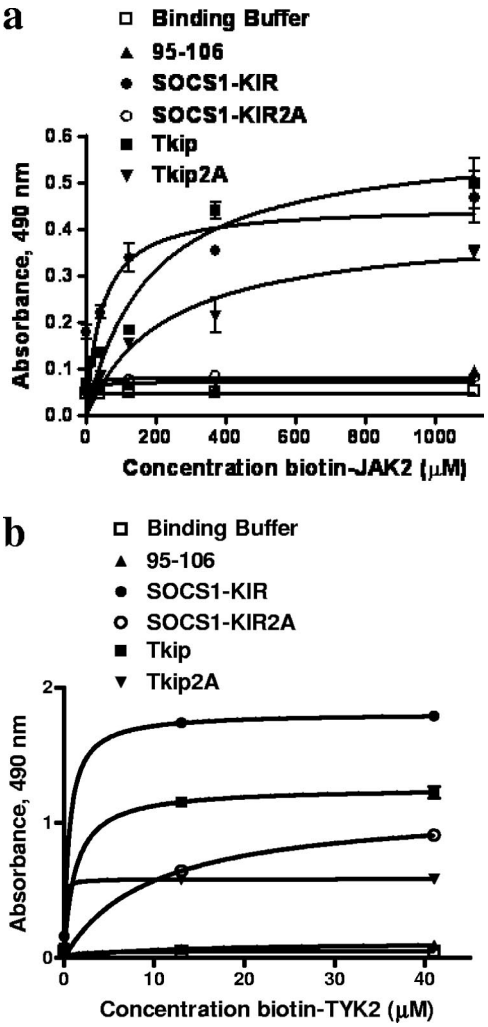

FIG. 2. SOCS1-KIR and Tkip bind to the autophosphorylation site peptides of JAK2 and TYK2. (a) SOCS1-KIR binds to JAK2 autophosphorylation site peptide JAK2(1001-1013). SOCS1-KIR, SOCS1-KIR2A (alanines substituted for phenylalanines at positions 56 and 59 of SOCS1-KIR), Tkip, Tkip2A, and a control peptide were immobilized in 96-well plates at 3 μg/well. Following blocking, various concentrations of biotinylated JAK2(1001-1013) peptide were added and the plates were incubated for 1 h. Bound biotinylated JAK2(1001-1013) was detected with an avidin-neutravidin-HRP conjugate. Absorbance was measured with a standard plate reader. There were statistically significant differences between SOCS1-KIR and SOCS1-KIR2A ($P < 0.001$) and between Tkip and Tkip2A ($P < 0.001$), as determined by the Mann-Whitney signed-rank test. (b) SOCS1-KIR and Tkip bind in a dose-dependent manner to biotinylated TYK2 autophosphorylation site peptide. There were statistically significant differences between SOCS1-KIR and SOCS1-KIR2A ($P < 0.001$) and between Tkip and Tkip2A ($P < 0.001$), as determined by the Mann-Whitney signed-rank test. All of the binding assays were carried out in triplicate, and the data are representative of at least three independent experiments. Where there are no error bars, the values were essentially identical.

stitutions at positions 8 and 11 (Tkip2A), which correspond to possible sites of homology with KIR (13). SOCS1-KIR2A completely lost the ability to bind to any of the JAKs, which is consistent with previous studies of the requirement of residues 56 and 59 for SOCS-1 function (36). Importantly, these results further confirm the ability of SOCS1-KIR to bind to the autophosphorylation site of JAK2 and demonstrate the possible role of previously identified residues in SOCS-1 that are critical to its function. We have previously shown that Tkip recognized the JAK2 autophosphorylation site similarly to SOCS1-KIR but not in precisely the same manner (33). Tkip2A showed reduced binding to JAK2 and TYK2 compared to Tkip. As indicated, Tkip binding to these two kinases was similar to that of SOCS1-KIR.

SOCS1-KIR mimetic binds to JAK2 and TYK2 in an anti-SOCS1-KIR ELISA. It has been suggested that the KIR of SOCS-1 functions as a pseudosubstrate rather than by binding to the activation loop of JAK2, as we have previously reported (33) and shown above in the biotinylation ELISA. Accordingly, we immunized rabbits with SOCS1-KIR conjugated to keyhole limpet hemocyanin and used a standard ELISA approach for detection of SOCS1-KIR binding to JAK2 and TYK2 activation loop sites to confirm the above bindings. The binding curve for the specificity of anti-SOCS1-KIR binding to SOCS1-KIR is shown in Fig. 3a. SOCS1-KIR, but not SOCS1-KIR2A, bound to the anti-SOCS1-KIR antibody. As shown in Fig. 3b, SOCS1-KIR bound to JAK2 and TYK2, similar to the binding in the biotinylation ELISA of Fig. 2. The fact that the anti-SOCS1-KIR antibody did not recognize SOCS1-KIR2A precluded binding assays with this mutant by this approach. Certainly, the agreement between JAK2 and TYK2 binding in the two ELISA approaches, along with the absence of SOCS1-KIR2A binding of Fig. 2, supports results indicating that the KIR of SOCS-1 recognizes the activation loops of JAK2 and TYK2. This does not preclude the possible recognition of other regions or domains of the JAKs. The binding results are important in the context of the mechanism of SOCS-1 mimetic inhibition of vaccinia virus replication in culture and protection of mice against lethal vaccinia virus infection as presented below.

Tkip and SOCS1-KIR inhibition of STAT phosphorylation. As a functional correlate of the binding of Tkip and SOCS1-KIR to the autophosphorylation site of the JAK kinases, we stimulated cells with IFN-γ and the type I IFN IFN-τ. IFN-γ interaction with its receptor activates JAK1 and JAK2, which are responsible for phosphorylation of STAT1α (19). Like other type I IFNs, IFN-τ activates JAK1 and TYK2, which phosphorylate STAT1α, STAT2, STAT3, and probably other STATs (8). As previously reported (33), both lipo-Tkip and lipo-SOCS1-KIR inhibited the IFN-γ-induced phosphorylation of STAT1α in fibroblast cells (Fig. 4a), which is consistent with binding to JAK2 by both peptides. IFN-τ caused phosphorylation of STAT1α and STAT3 in mouse L929 cells and STAT2 in WISH cells, all of which were inhibited by Tkip and SOCS1-KIR (Fig. 4b), which is consistent with the recognition of TYK2 by both peptides. WISH cells were used here because of the availability of the relevant antibody. The ability of Tkip and SOCS1-KIR to inhibit relevant STAT activation is consistent with their binding to the activation loop of the JAKs.

SOCS1-KIR and Tkip require previously identified amino acid residues for inhibition of STAT1α phosphorylation involving TYK2. We next determined the ability of SOCS1-KIR2A and Tkip2A to inhibit IFN-τ-induced activation of STAT1α in cells. As shown in Fig. 4c, lipophilic SOCS1-KIR2A (lipo-SOCS1-KIR2A) failed to inhibit IFN-τ-induced activation of STAT1α in L929 cells, in contrast to the

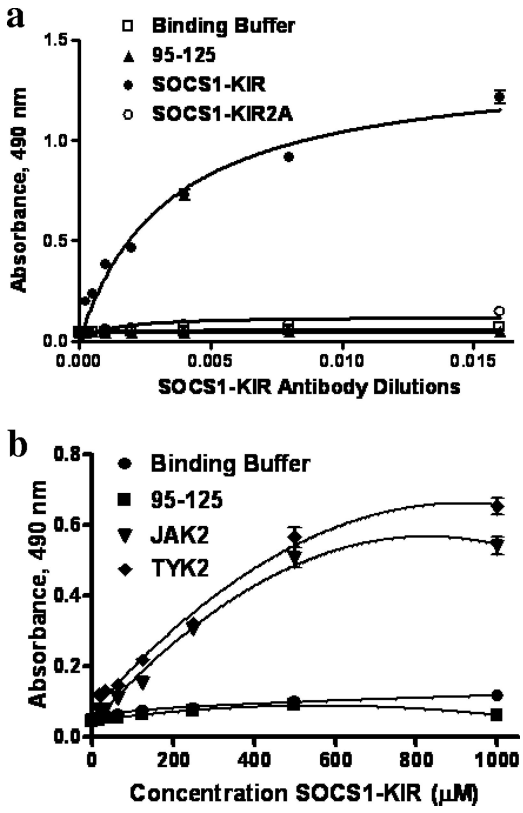

FIG. 3. SOCS1-KIR binding to autophosphorylation site peptides JAK2 and TYK2 as determined by an antibody ELISA. (a) SOCS1-KIR antibody is specific for the SOCS1-KIR peptide. SOCS1-KIR, SOCS1-KIR2A, and a control peptide were immobilized on a 96-well plate at 3 μg/well. Following blocking, various dilutions of SOCS1-KIR antibody were added and the plate was incubated for 1 h. Bound antibody was detected with a goat anti-rabbit IgG-HRP conjugate, followed by the addition of OPD substrate and 2N H_2SO_4. Absorbance was measured with a standard plate reader. (b) SOCS1-KIR binds to JAK2 and TYK2 autophosphorylation site peptides. JAK2, TYK2, and a control peptide were immobilized in a 96-well plate at 3 μg/well. Following blocking, various concentrations of SOCS1-KIR were added and the plate was incubated for 1 h. SOCS1-KIR antibody was added for 1 h of incubation, and bound SOCS1-KIR was detected as described for panel a.

lipophilic wild-type peptide, reflecting a lack of recognition of TYK2. Lipophilic Tkip2A also did not inhibit IFN-τ-induced activation of STAT1α. Thus, SOCS1-KIR2A and Tkip2A showed a loss of functional activity consistent with reduced recognition of the relevant JAKs. The binding and functional results obtained with SOCS1-KIR, Tkip, and their alanine substitution mutant forms further support our previous demonstration that they recognized the autophosphorylation sites of JAKs (33).

SOCS1-KIR and Tkip protect mice against a lethal dose of vaccinia virus. Vaccinia virus is a prototype poxvirus, and its lethal infectivity of mice was blocked by the tyrosine kinase inhibitors Gleevec (Abl) (28) and CI-1033 (ErbB-1) (35). We therefore examined SOCS1-KIR and Tkip, given their inhibitory effects on JAK2 and ErbB-1 (13, 14, 33), for the ability to protect mice challenged with a lethal dose of the Western Reserve strain of vaccinia virus. C57BL/6 mice were treated

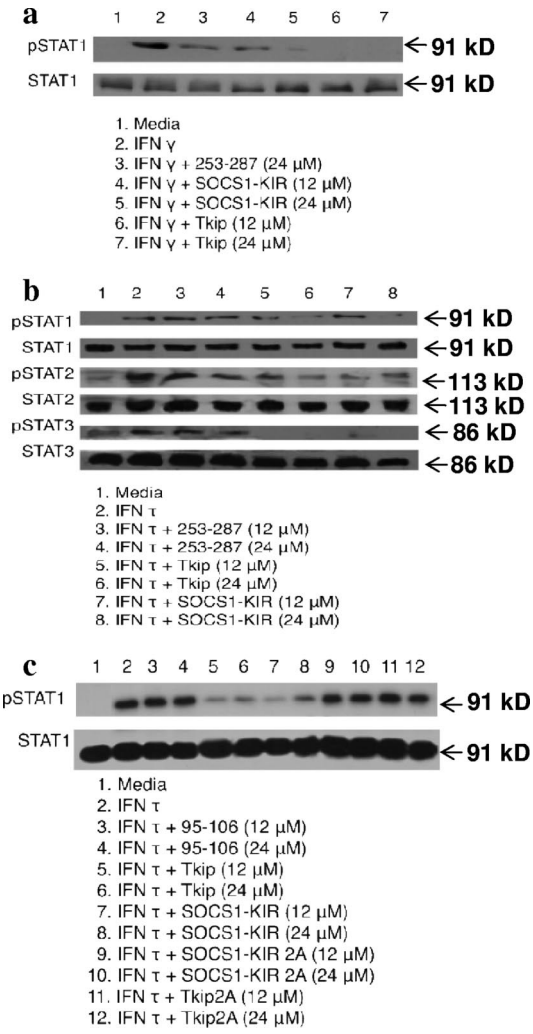

FIG. 4. Kinase inhibition patterns of SOCS1-KIR and Tkip in STAT1, STAT2, and STAT3 phosphorylation. (a) SOCS1-KIR and Tkip inhibit IFN-γ-induced STAT1 activation in L929 cells. L929 cells were seeded onto six-well plates at 1×10^6 cells/well and pretreated with medium alone, lipo-Tkip, lipo-SOCS1-KIR, or a control peptide for 2 h at 37°C. Following 2 h of incubation in the presence or absence of IFN-γ (4,000 U/ml), the cells were washed and lysed. Whole-cell extracts were resolved by 12% SDS-PAGE, transferred to nitrocellulose membrane, and examined with pSTAT1 (pY^{701}) antibody. The membrane was stripped and reprobed with STAT1 antibody. (b) SOCS1-KIR and Tkip inhibit IFN-τ-induced STAT1 and STAT3 activation in L929 cells and STAT2 activation in WISH cells. WISH cells were used here because of the availability of reagents. L929 cells were seeded into six-well plates at 1×10^6/well and pretreated with medium alone, lipo-Tkip, lipo-SOCS1-KIR, or a control peptide for 2 h at 37°C. WISH cells were seeded onto six-well plates at 2.5×10^5/well and pretreated with medium alone, lipo-Tkip, lipo-SOCS1-KIR, or a control peptide for 2 h at 37°C. Following 2 h of incubation in the presence or absence of IFN-τ (10,000 U/ml), the cells were washed and lysed. Whole-cell extracts were resolved by 12% SDS-PAGE, transferred to nitrocellulose membrane, and examined with antibodies to pSTAT1 (pY^{701}), pSTAT2 (pY^{690}), or pSTAT3 (pY^{705}). The membrane was stripped and reprobed with STAT1, STAT2, or STAT3 antibody. (c) SOCS1-KIR2A and Tkip2A do not inhibit IFN-τ-induced STAT1 activation in L929 cells. L929 cells were seeded onto six-well plates at 1×10^6/well and pretreated with medium alone, lipo-SOCS1-KIR, lipo-SOCS1-KIR2A, lipo-Tkip, lipo-Tkip2A, or a control peptide for 2 h at 37°C. Following 2 h of incubation in the presence or absence of IFN-τ (10,000 U/ml), the cells were washed and lysed. Whole-cell extracts were resolved by 12% SDS-PAGE, transferred to nitrocellulose membrane, and examined with pSTAT1 (pY^{701}) antibody. The membrane was stripped and reprobed with STAT1 antibody.

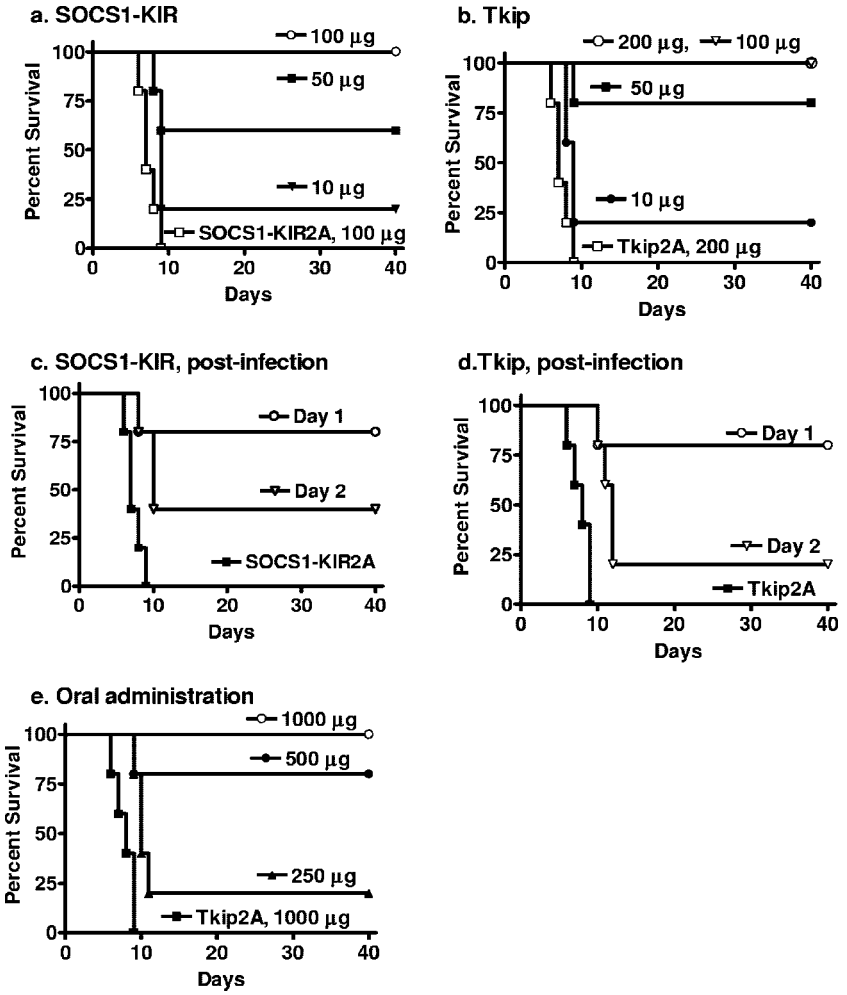

FIG. 5. SOCS1-KIR and Tkip protect mice against intranasal challenge with vaccinia virus. (a) SOCS1-KIR. Mice (C57BL/6, $n = 5$ per group in all mouse experiments) were pretreated i.p. on days −2, −1, and 0 with 100 μg (○), 50 μg (■), or 10 μg (▼) of lipo-SOCS1-KIR peptide or 100 μg (□) of control peptide lipo-SOCS1-KIR2A. On day 0, vaccinia virus (2×10^6 PFU) was administered intranasally. Survival of mice was followed for 40 days. The significance of differences between different treatments was measured by the log rank survival method, which gave *P* values of 0.002, 0.002, and 0.005 for the administration of 100, 50, and 10 μg of lipo-SOCS1-KIR versus the control peptide, respectively. (b) Tkip. Mice were pretreated on days −2, −1, and 0 with 200 μg (○), 100 μg (▽), 50 μg (■), or 10 μg (●) of lipo-Tkip or 200 μg of the lipo-Tkip2A control (□). Infection with vaccinia virus was similar to that in panel a. Postinfection treatment with lipo-SOCS1-KIR or lipo-Tkip provides partial protection against vaccinia virus infection. (c) Postinfection lipo-SOCS1-KIR treatment. Mice ($n = 5$) were infected intranasally with 2×10^6 PFU of vaccinia virus on day 0. Starting at day 1 (○) or 2 (▽) after infection, mice were treated i.p. with 200 μg of lipo-SOCS1-KIR for 3 consecutive days. Control peptide lipo-SOCS1-KIR2A (■) at 200 μg was administered on days −2, −1, and 0. Survival was followed for 40 days. *P* values for the significance of differences between lipo-SOCS1-KIR treatment on days 1 and 2 versus the control peptide lipo-SOCS1-KIR2A were 0.002 and 0.005, respectively. (d) Postinfection lipo-Tkip treatment. Mice were infected with vaccinia virus in a manner similar to that described for panel a. Starting at day 1 (○) or 2 (▽) after infection, mice were treated i.p. with 200 μg of lipo-Tkip for 3 consecutive days. Control peptide lipo-Tkip2A (■) at 200 μg was administered on days −2, −1, and 0. Survival was followed for 40 days. *P* values for the significance of differences between lipo-Tkip treatment on days 1 and 2 versus the control lipo-Tkip2A were 0.002 and 0.005, respectively. (e) Oral treatment with lipo-Tkip protects mice against intranasal challenge with vaccinia virus. Mice ($n = 5$) were given 1,000 μg (○), 500 μg (●), or 250 μg (▲) of lipo-Tkip on days −2, −1, and 0 by the oral route. One thousand micrograms of a control peptide, lipo-Tkip2A (■), was given orally on the same days. On day 0, 2×10^6 PFU of vaccinia virus was administered intranasally. Survival of mice was followed for 40 days. *P* values for the significance of differences between 1,000, 500, and 250 μg of lipo-Tkip and the control peptide were 0.002, 0.008, and 0.008, respectively.

with 10, 50, and 100 μg of lipo-SOCS1-KIR on days −2, −1, and 0 by i.p. injection. On day 0, the mice were challenged intranasally with 2×10^6 PFU of vaccinia virus, which is approximately 100 50% lethal doses (Fig. 5a). Complete protection was observed with 100 μg of lipo-SOCS1-KIR, whereas 50 and 10 μg of lipo-SOCS1-KIR resulted in 60 and 20% protection from death, respectively. The amounts of the SOCS1-KIR peptide used, at 100, 50, and 10 μg per mouse, correspond to 5, 2.5, and 0.5 mg/kg body weight. Mice that recovered were completely free of any disease symptoms for the 40 days they were observed. The lipophilic palmitate group was previously shown to be required for penetration of the cell membrane (13). The control peptide lipo-SOCS1-KIR2A, in which the phenylalanines at residues 56 and 59 were replaced with alanines, did not protect the mice at 100 μg, and 100% death occurred between days 6 and 9. Similarly, lipo-Tkip was used to

pretreat mice on days −2, −1, and 0 and the mice were infected intranasally on day 0 with 2×10^6 PFU of vaccinia virus. Mice were completely protected by pretreatment with 100 μg and 200 μg, whereas with 50 μg and 10 μg of Tkip, 80% and 20% protection was observed (Fig. 5b). The amounts of Tkip used, at 200, 100, 50, and 10 μg per mouse, correspond to 10, 5, 2.5, and 0.5 mg/kg body weight. A lipophilic control peptide with alanine substitutions at positions 8 and 11, Tkip2A, at 200 μg per mouse, did not show any protection, providing evidence of the specificity of action of Tkip. Treatment of L929 cells and murine splenocytes with up to 100 μM SOCS-1 mimetics and determination of dehydrogenase enzymes in viable cells by MTS assay revealed the absence of any cytotoxic effect in these peptides (data not shown). Thus, both lipo-SOCS1-KIR and lipo-Tkip were able to completely protect mice against a highly lethal dose of vaccinia virus.

SOCS1-KIR and Tkip rescue mice from ongoing lethal vaccinia virus infection. We were interested in determining the ability of lipo-SOCS1-KIR and lipo-Tkip to rescue mice from ongoing virus infection. Accordingly, mice were infected intranasally with 2×10^6 PFU of vaccinia virus, a dose at which 100% death occurs by day 9. Two hundred micrograms of lipo-SOCS1-KIR peptide was injected i.p. for 3 consecutive days beginning at day 1 or 2 after challenge with vaccinia virus. Therapy initiated at day 1 postinfection resulted in 80% protection, while therapy begun on day 2 resulted in 40% protection (Fig. 5c). Mice treated i.p. on days −2, −1, and 0 with control peptide lipo-SOCS1-KIR2A, in which the phenylalanines at residues 56 and 59 were replaced with alanines, all died by day 9. The mice that recovered remained healthy for the 40 days of the experiment. Similarly, 200 μg of lipo-Tkip, given i.p. for 3 consecutive days beginning at day 1, had significant, 80%, therapeutic efficacy, which declined to 20% by day 2 of postinfection therapy (Fig. 5d). Mice treated i.p. on days −2, −1, and 0 with control peptide lipo-Tkip2A, in which the phenylalanines at residues 8 and 11 were replaced with alanines, all died by day 9. Therefore, when administered 1 day after infection, both lipo-SOCS1-KIR and lipo-Tkip possessed therapeutic efficacy against an ongoing infection with an overwhelming lethal dose of virus. This postinfection therapeutic benefit is less than that of the IFN mimetic peptide we have described earlier, where treatment at up to 5 days postinfection resulted in 80% protection (3). Compared to Gleevec and CI-1033, however, where there was no demonstrable postinfection protection, lipo-SOCS1-KIR and lipo-Tkip appear to be more effective therapeutics (28, 35).

Orally administered lipo-Tkip protects mice against intranasal challenge with vaccinia virus. We next addressed the issue of whether the SOCS-1 mimetic lipo-Tkip, when administered orally, was protective against an intranasal vaccinia virus challenge. Accordingly, we administered 250 to 1,000 μg of lipo-Tkip per mouse (corresponding to 12.5 to 50 mg/kg body weight) or 1,000 μg of the control lipo-Tkip2A orally to mice via feeding needles at days −2, −1, and 0, after which the mice were challenged intranasally with 10^6 PFU of vaccinia virus on day 0 (Fig. 5e). Mice were completely protected from death by 1,000 μg of lipo-Tkip, whereas 500 and 250 μg of lipo-Tkip resulted in 80 and 20% protection, respectively. The control lipo-Tkip2A-fed mice were all dead by day 9. The oral administration did not involve special treatments such as the use of liposomes for delivery or raising the pH to protect against acid proteases. These results, therefore, provide proof of the concept that lipo-Tkip is protective against intranasal vaccinia virus even when administered orally. Similar results were obtained with SOCS1-KIR (data not shown).

TABLE 2. Virus levels in tissues of mice treated with Tkip and Tkip2A and challenged with vaccinia virus[a]

Tissue	No. of PFU of virus after treatment with:	
	Tkip	Tkip2A
Trachea	<LOD[b]	$9.5 \times 10^3 \pm 0.7 \times 10^3$
Lung	<LOD	$15 \times 10^3 \pm 1.0 \times 10^3$
Spleen	<LOD	$2.5 \times 10^3 \pm 0.3 \times 10^3$
Brain	<LOD	$30 \times 10^3 \pm 2.0 \times 10^3$

[a] Mice ($n = 3$) on day 6 after i.p. administration of lipo-Tkip or lipo-Tkip2A and intranasal challenge with vaccinia virus were sacrificed, and organs were harvested, homogenized, and used to assay vaccinia virus.
[b] <LOD, below the limit of detection (100 PFU per organ).

Comparison of vaccinia virus levels in tissues of mice protected with the SOCS-1 mimetic versus those treated with a control peptide. Related to the protective effect of the SOCS-1 mimetic, we determined the virus loads of selected organs at day 6 after an intranasal challenge of mice with 2×10^6 PFU of vaccinia virus. As shown in Table 2, mice treated with the control lipo-Tkip2A contained high virus levels in the respiratory system, 9.5×10^3 PFU in the trachea and 15×10^3 PFU in the lungs. The spleen had 2.5×10^3 PFU. Owing to the neurotropic properties of the Western Reserve strain of vaccinia virus, 30×10^3 PFU were observed in the brain. Lipo-Tkip-treated mice, however, did not have any detectable vaccinia virus in any of these organs at day 6. This suggests that the SOCS-1 mimetic is very effective at inhibiting vaccinia virus replication in vivo, which is consistent with the effective protection of mice against the lethal effects of the virus.

Tkip and SOCS1-KIR inhibit vaccinia virus replication, as determined by a one-step growth curve experiment. In order to obtain more insight into the effects of Tkip and SOCS1-KIR on vaccinia virus replication, we carried out a one-step growth curve experiment. BSC-40 cells that were treated with lipo-Tkip or lipo-SOCS1-KIR at 50 μM were infected with vaccinia virus at an MOI of 5 to ensure simultaneous infection of all of the cells for a one-step growth curve experiment. An IFN-γ mimetic designated lipo-IFN-γ(95-132), which has previously been shown to inhibit vaccinia virus replication, was used as a positive control (1, 3). Alanine substitution-containing mutant forms of SOCS1-KIR and Tkip were used as controls. Both lipo-Tkip and lipo-SOCS1-KIR inhibited virus replication at both the intracellular (Fig. 6a) and extracellular (Fig. 6b) levels, as assessed by virus yield plaque assay. The virus yield at 24 h after infection shown in Fig. 6 is also presented in Table 3. Lipo-SOCS1-KIR inhibited the intracellular virus yield by 83% and the extracellular virus yield by 90%. Similarly, Tkip inhibited the intracellular virus yield by 82% and the extracellular yield by 91%. SOCS1-KIR2A failed to inhibit the vaccinia virus yield both intracellularly and extracellularly. Similarly, lipo-Tkip2A failed to inhibit vaccinia virus replication. Thus, the results of Fig. 6 and Table 3 indicate that the SOCS-1 mimetics inhibit vaccinia virus replication and not simply virus release. The fact that alanine substitutions for phenylalanine at

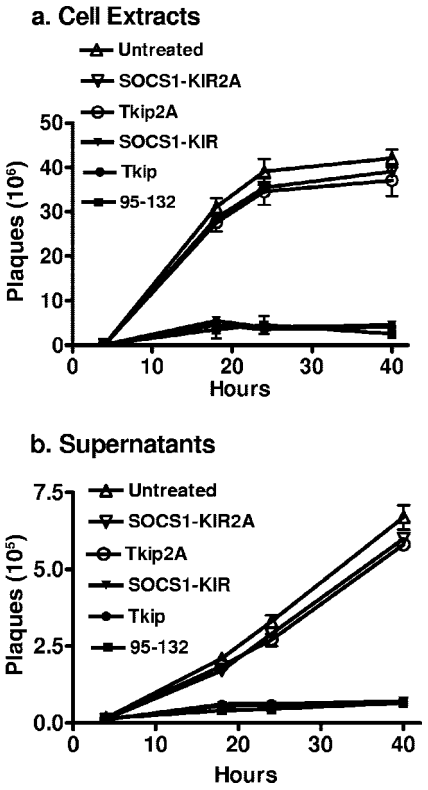

FIG. 6. One-step growth curve of inhibition of vaccinia virus replication by SOCS1-KIR and Tkip. BSC-40 cells grown to confluence were left untreated or treated with lipo-SOCS1-KIR, lipo-Tkip, or their alanine substitution-containing mutant forms at 50 μM for 1 h. For a positive control, an IFN-γ mimetic spanning residues 95 to 132 (designated 95-132) that was previously shown to inhibit vaccinia virus replication (1, 3) was used. Cells were then infected with vaccinia virus at an MOI of 5 for 1 h, after which the cells were washed and incubated in the presence of the same concentrations of peptides for the indicated times. The cell extracts (a) and supernatants (b) obtained were titrated for the amounts of intracellular and extracellular virus, respectively. Note the difference of the scale on the *y* axis, indicating that there is less extracellular virus than intracellular virus.

previously identified critical residues resulted in loss of inhibition of vaccinia virus replication is evidence of both the specificity and virus entry of the SOCS-1 mimetic-treated cells.

To test for a concentration dependence of the effect of lipo-SOCS1-KIR and lipo-Tkip, increasing concentrations of these peptides were added to the cells, followed by infection with vaccinia virus at an MOI of 5, and the intracellular (Fig. 7a and c) and extracellular (Fig. 7b and d) virus levels were quantitated 24 h after infection. With 1, 5, 10, and 25 μM SOCS1-KIR, levels of 61%, 42%, 21%, and 12% of the control intracellular virus level and 53%, 31%, 17%, and 11% of the control extracellular virus level, respectively, were observed. Alanine substitution-containing mutant forms at 25 μM did not affect the intracellular or extracellular virus level produced (Fig. 7a to d). A similar profile was observed with Tkip treatment (Fig. 7c and d). A 50% effective dose of less than 5 μM lipo-SOCS1-KIR or lipo-Tkip for the replication of vaccinia virus in BSC-40 cells was observed. Thus, the SOCS-1 mimetics inhibited vaccinia virus replication.

Adaptive immunity to vaccinia virus in mice treated with Tkip. Mice protected by lipo-Tkip were rechallenged 10 weeks later with a second dose of 10^6 PFU of vaccinia virus administered intranasally without additional Tkip treatment. All five mice in the rechallenged group were protected against the lethality of the virus without showing symptoms of distress (Fig. 8a). Naïve control mice all died by day 9. Thus, the mice treated with the SOCS-1 mimetic lipo-Tkip were not inhibited in the development of protective immunity from the first challenge with vaccinia virus. Similar results were obtained with mice protected by SOCS1-KIR (data not shown).

Splenocytes obtained 2 and 3 weeks after virus challenge from protected mice underwent antigen-specific proliferation with stimulation indices of 4 to 5 (Fig. 8b). Cells from control mice did not respond to vaccinia virus. The proliferation results suggest the induction of virus-specific $CD4^+$ T cells. Splenocytes were also tested for production of the cytokine IFN-γ by ELISPOT assay. Similar to the proliferative response, CD4-depleted splenocytes showed increased secretion of IFN-γ by ELISPOT at 2 and 3 weeks (Fig. 8c), suggesting the induction of vaccinia virus-specific cytotoxic $CD8^+$ T cells. Control cells did not respond to virus.

Sera from protected mice were examined for antibodies at 1 to 4 weeks. As shown in Fig. 8d, IgA antibodies peaked at 2 weeks but were significant out to 4 weeks postinfection, while the IgG antibody response peaked over 2 to 4 weeks after challenge (Fig. 8e). The IgA antibodies are particularly relevant to the intranasal route of virus challenge. The antibody response also resulted in the production of neutralizing antibodies, which peaked in the second week and probably involved both IgA and IgG antibodies to vaccinia virus, as shown in Fig. 8f. Thus, mice protected by lipo-Tkip mounted strong cellular and humoral immune responses to vaccinia virus.

Vaccinia virus-induced ErbB-1 and JAK2 phosphorylation is inhibited by Tkip and SOCS1-KIR. Since poxviruses have been shown to activate cellular tyrosine kinases such as ErbB-1 and JAK2 early in the infection of cells, we tested the effect of the SOCS-1 mimetic Tkip on vaccinia virus-induced phosphorylation of ErbB-1 and JAK2. Such activation has been shown to play a role in virus spread from cell to cell. BSC-40 cells were left untreated or pretreated with 20 μM lipo-Tkip or a

TABLE 3. Inhibition of vaccinia virus yield by SOCS1-KIR and Tkip[a]

Treatment	Virus yield (10^5)		% of control	
	Intracellular	Extracellular	Extracellular	Intracellular
None	390 ± 29.0	3.3 ± 0.2		
SOCS1-KIR	40 ± 3.0	0.57 ± 0.03	10.2	17
SOCS1-KIR2A	354 ± 30.0	2.9 ± 0.01	90.7	88
Tkip	35 ± 2.5	0.62 ± 0.04	8.9	18
Tkip2A	345 ± 30	2.7 ± 0.2	81	82
IFN-γ(95-132)	45 ± 5.0	0.45 ± 0.04	11.5	13

[a] A single-step assay of vaccinia virus yield was performed on confluent BSC-40 cells infected with virus at an MOI of 5. The peak virus yield after 24 h of infection, as shown in Fig. 6, was used for calculations. Peptides were used at a final concentration of 50 μM. The experiment was carried out in triplicate and repeated twice with similar results. There was a statistically significant difference between the lipo-SOCS1-KIR and lipo-Tkip treatments versus no treatment ($P < 0.001$), while the results obtained with the mutant forms were not significantly different by the Mann-Whitney signed-rank test.

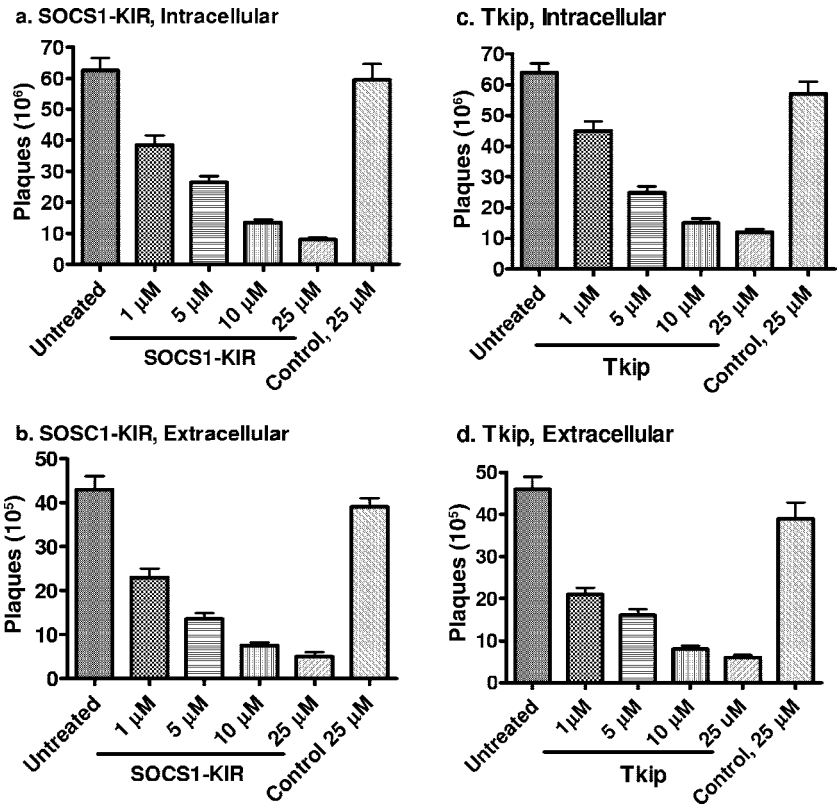

FIG. 7. SOCS1-KIR and Tkip inhibit vaccinia virus replication in a dose-dependent manner. BSC-40 cells were grown to confluence and left untreated or treated with the indicated amounts of lipo-SOCS1-KIR (a and b) or lipo-Tkip (c and d) for 1 h. Control peptides lipo-SOCS1-KIR2A (a and b) and lipo-Tkip2A (c and d) were used at 25 μM. Cells were next infected with vaccinia virus at an MOI of 5. After 1 h, the cells were washed and incubated in the presence of the same concentrations of peptides for 1 day. The supernatants and cell extracts obtained were titrated for the amounts of intracellular (a and c) and extracellular (b and d) virus, respectively.

control peptide for 30 min, followed by infection with vaccinia virus (Fig. 9). Immunoprecipitation with phosphotyrosine antibodies of cell extracts 1 and 5 min after infection with vaccinia virus, followed by Western blot analysis with ErbB-1 and JAK2 antibodies, revealed that the phosphorylation of both tyrosine kinases was significantly inhibited by lipo-Tkip. Lipo-SOCS1-KIR similarly inhibited ErbB-1 and JAK2 activation (data not shown). Thus, consistent with its inhibition of vaccinia virus replication, lipo-Tkip and lipo-SOCS1-KIR inhibited virus-induced activation of ErbB-1 and JAK2.

Tkip and SOCS1-KIR inhibit vaccinia virus transcription and replication at early, intermediate, and late stages of infection. The one-step growth curve results indicate that the SOCS-1 mimetics inhibited vaccinia virus replication. We performed real-time PCR on early (D12L), intermediate (A1L), and late (A7L) gene expression in order to determine the stage of virus replication that was inhibited by lipo-Tkip and lipo-SOCS1-KIR. As shown in Fig. 10a to c, lipo-Tkip and lipo-SOCS1-KIR, but not lipo-Tkip2A or lipo-SOCS1-KIR2A, inhibited D12L, A1L, and A7L transcription by real-time quantitative PCR. Actin mRNA levels were quantitated under the same conditions and used to determine the relative amounts of different transcripts. D12L, A1L, and A7L code for the small subunit of mRNA capping enzyme, a late transcription factor, and the large subunit of early gene transcription factor VETF, respectively. An overall decrease in transcription may contribute to the decreased replication of the virus. The results indicate that the mimetics inhibited vaccinia virus transcription, as determined by the analysis of transcripts from the early and possibly later stages of growth.

We next added lipo-Tkip, lipo-SOCS1-KIR, and their alanine substitution-containing variants to BSC-40 cells infected with vaccinia virus at an MOI of 5 at 0, 1, 2, and 4 h postinfection. As shown in Fig. 11a to d for intracellular levels of vaccinia virus and Fig. 11e to h for extracellular levels of vaccinia virus, Tkip and SOCS1-KIR inhibited vaccinia virus replication when these SOCS-1 mimetics were added from 0 to 4 h postinfection. This finding is in contrast to a recent study with aurintricarboxylic acid, where virus replication was inhibited at 0 h, but not at 1 h, postinfection (24). In the cases of the tyrosine kinase inhibitors Gleevec (Abl kinase [28]) and CI-1033 (EGF receptor [35]), there was no inhibition of virus replication, but rather inhibition of the release of mature virions from the plasma membrane of the infected cells. Thus, the SOCS-1 mimetics inhibit virus transcription and replication beyond the initial stages of infection, which probably helps explain their potent anti-vaccinia virus effects.

DISCUSSION

Recently, it was shown that inhibitors of key cellular tyrosine kinases could reduce the virulence and lethality of poxvirus infection (28, 35), which suggests a novel approach to thwart-

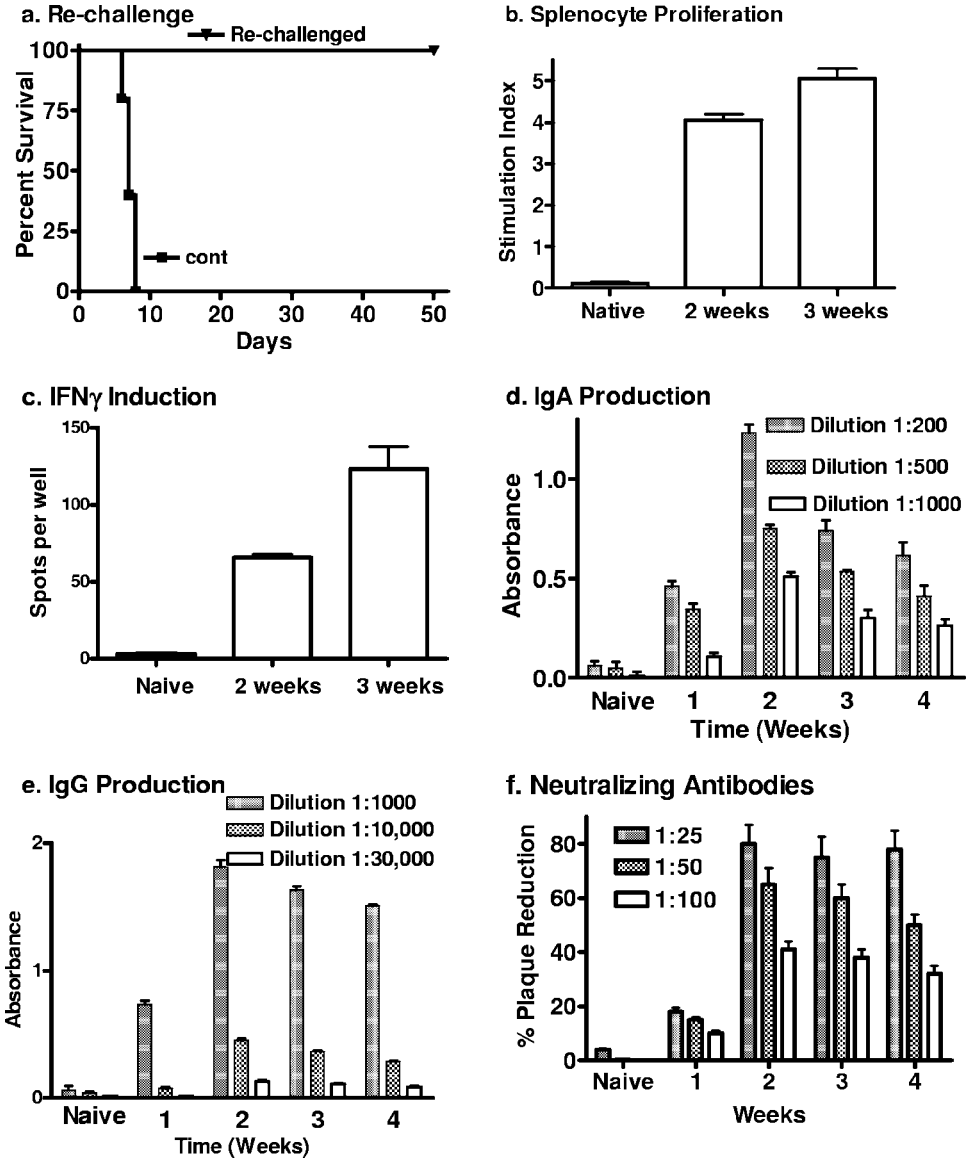

FIG. 8. Adaptive immune response in mice that recovered from vaccinia virus infection with lipo-Tkip treatment. (a) Survival of mice after a rechallenge with vaccinia virus. Naïve mice (■; $n = 5$) and those that had recovered from vaccinia virus infection with lipo-Tkip treatment for 30 days (▼) were infected intranasally with 2×10^6 PFU of vaccinia virus in 10 μl. Survival was followed for 50 days. The significance of the difference, as measured by log rank survival, was $P = 0.0002$ for the rechallenged group versus the naïve mice. (b) Cell-mediated immune response in mice that recovered from vaccinia virus infection with lipo-Tkip treatment. Splenocytes (10^5) obtained from naïve mice or mice that recovered ($n = 3$) 2 or 3 weeks after infection and lipo-Tkip treatment were incubated with UV-inactivated, purified vaccinia virus. Four days later, [^{3}H]thymidine was added for 8 h of incubation and its incorporation was followed. The stimulation index is the incorporation into splenocytes cultured with test antigen divided by the incorporation into splenocytes cultured with medium alone. Averages and standard deviations are shown. (c) Vaccinia virus-specific response in CD4-depleted splenocytes by ELISPOT analysis. Splenocytes obtained from naïve mice or mice that recovered ($n = 3$) 2 or 3 weeks after infection with lipo-Tkip treatment were depleted of CD4 cells, and 10^5 cells thus obtained were incubated in microtiter plates previously coated with antibody to IFN-γ in the presence of vaccinia virus (MOI = 0.01). After 2 days of incubation, the spots (IFN-γ-secreting cells) per well were counted. The values shown are averages and standard deviations. (d and e) Presence of vaccinia virus-specific antibodies in mice that recovered from infection with lipo-Tkip treatment. Sera collected from naïve mice ($n = 3$) or those that recovered from vaccinia virus infection with lipo-Tkip treatment were collected in the weeks indicated. Sera were diluted as indicated and added to wells of microtiter plates coated with UV-inactivated vaccinia virus. After washing to remove nonspecific binding, secondary anti-mouse IgA (d) or IgG (e) antibody conjugated to HRP was added, followed by the addition of OPD substrate and absorption measurement. The values shown are averages and standard deviations. (f) Neutralizing antibodies in mice that recovered. Sera taken from naïve mice ($n = 3$) or those that recovered from vaccinia virus infection with lipo-Tkip treatment in the weeks indicated were diluted as shown, mixed with vaccinia virus (100 PFU), incubated for 1 h, and then added to BSC-40 cells. One hour later, regular growth medium was added to the cells and the mixture was incubated for 2 days. The reduction in the number of plaques is shown as a percentage and the standard deviation.

ing the pathogenicity of these viruses. Specifically, the Abl tyrosine kinase inhibitor Gleevec protected mice against lethal vaccinia virus infection (28), while the EGF receptor ErbB-1 inhibitor CI-1033 similarly protected mice against vaccinia virus (35). Neither kinase inhibitor interfered with vaccinia virus replication, but Gleevec inhibited the release of EEV from actin tails (28). Vaccinia virus and variola virus code for EGF-like growth factors called VGF and SPGF, respectively (9, 10,

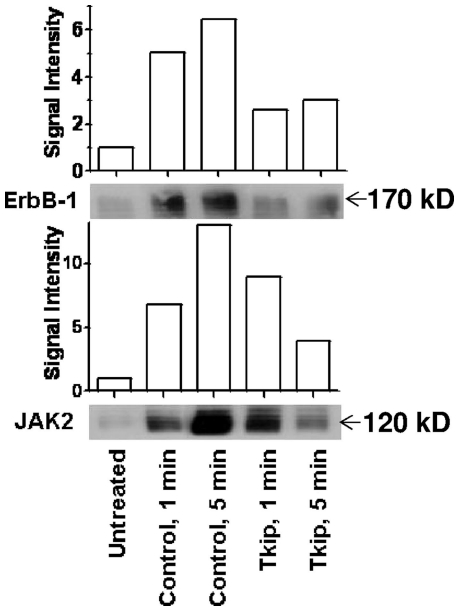

FIG. 9. Vaccinia virus-induced phosphorylation of ErbB-1 and JAK2 is inhibited by Tkip. Extracts of BSC-40 cells left untreated or pretreated for 30 min with 20 μM lipo-Tkip or control peptide lipo-Tkip2A and infected with vaccinia virus (MOI = 0.1) for 1 or 5 min were harvested and immunoprecipitated with phosphotyrosine antibody. Phosphotyrosine proteins were electrophoresed and probed with antibodies to ErbB-1 or JAK2.

17). These growth factors act on ErbB-1 and are important for virus replication and release (9, 17, 32). In this regard, the kinase inhibitors, through their action on ErbB-1, may block downstream effects of ErbB-1 by inactivating other kinases such as Src. It is worth noting that deletion of the VGF gene from its genome resulted in decreased pathogenicity in vivo and reduced its 50% lethal dose by 2,000-fold (9). A similar role for the EGF homolog was observed in a myxoma virus-derived virus (26). There is evidence that the JAK/STAT signaling pathway is also involved in poxvirus replication. Tyrophostin AG490, an inhibitor of JAK2, as well as other tyrosine kinases, was shown to inhibit myxoma virus infection of a rabbit cell line (21). Myxoma virus induced phosphorylation of JAK1 and JAK2 with accompanying activation of STAT1α and STAT2 in infected cells. Both the JAK/STAT activations and infections were inhibited by AG490.

SOCS proteins are a family of inducible proteins that are negative regulators of cytokine, growth factor, and hormone signaling. There are eight identified members of the SOCS family, SOCS-1 to SOCS-7 and CIS (4, 11, 36). SOCS-1 is a negative regulator of cytokine, growth factor, and hormonal signaling that uses the JAK/STAT signaling pathway, as well as other tyrosine kinases such as the ErbB family of receptor tyrosine kinases (4, 11, 36). We have developed a small-peptide mimetic (Tkip) of SOCS-1 that, similar to SOCS-1, inhibits JAK2, as well as ErbB-1 kinase, activity (13, 14, 33). We have shown that a peptide corresponding to the KIR of SOCS-1, SOCS1-KIR, similarly inhibits JAK2 and ErbB-1 kinase activity (33). In assessing the JAK specificity of Tkip and SOCS1-KIR, we have shown that they bind to and inhibit the functions of JAK2 and TYK2. Thus, the SOCS-1 mimetic activity of Tkip

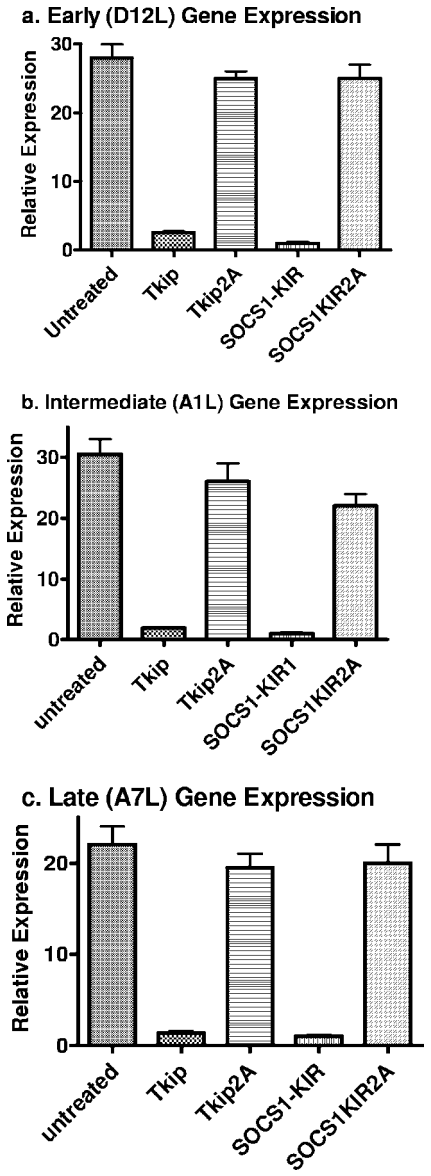

FIG. 10. Inhibition of vaccinia virus transcription by Tkip and SOCS1-KIR. BSC-40 cells mock treated or treated with lipo-Tkip, lipo-SOCS1-KIR, or alanine substitution-containing control peptides for 1 h were infected with vaccinia virus at an MOI of 5 for 1 h. The cells were washed and incubated in growth medium containing the same concentration of peptides for 18 h. RNA was extracted and used for cDNA synthesis, followed by quantitative PCR. The expression of early (D12L) (a), intermediate (AIL) (b), and late (A7L) (c) genes was compared with endogenous actin gene expression.

and SOCS1-KIR corresponds to the KIR sequence function of the SOCS-1 molecule. The inhibitory effect of the SOCS-1 mimetics on ErbB-1 and JAK2 are particularly dramatic early after vaccinia virus infection. Both ErbB-1 and JAK2 are strongly activated by 1 min postinfection with vaccinia virus, and the effect is enhanced by 5 min. The mimetics significantly inhibited this activation, which is consistent with inhibition of virus replication. This probably plays an important role in the protective effects of the SOCS-1 mimetics in vaccinia virus infection.

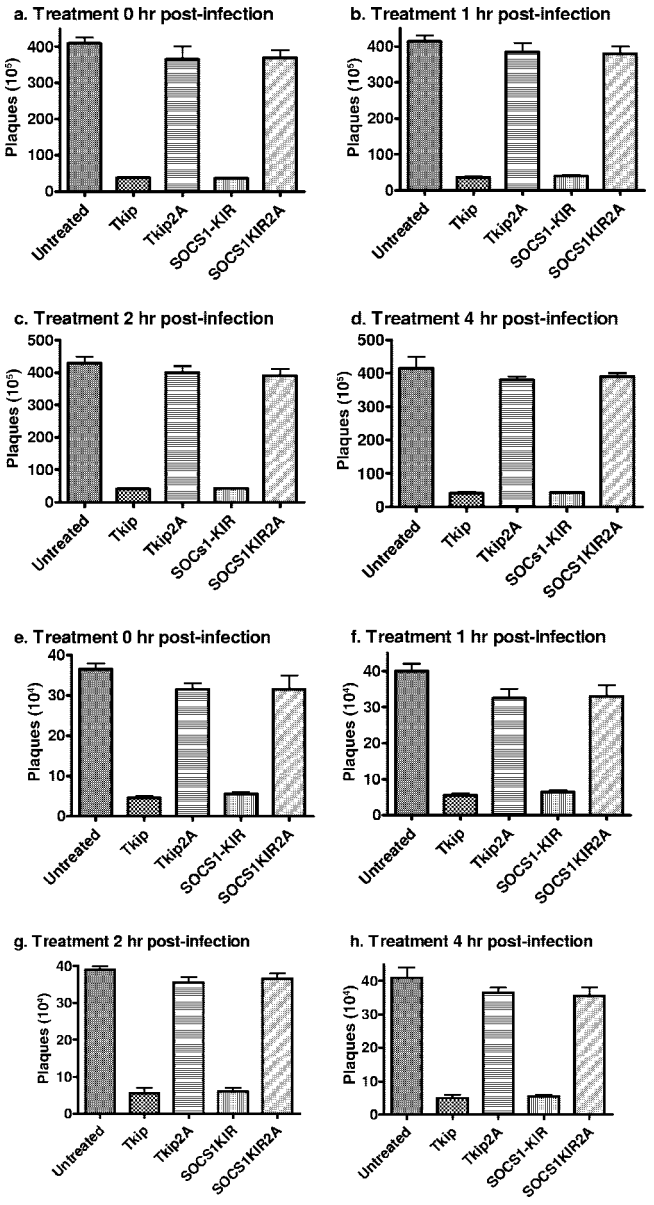

FIG. 11. Effect of SOCS1-KIR and Tkip treatment at different times on the replication of vaccinia virus. BSC-40 cells were infected with vaccinia virus at an MOI of 5 for 1 h. Cells were washed and treated with 25 μM lipo-SOCS1-KIR, lipo-Tkip, or the control peptides at time zero and 1 h, 2 h, and 4 h after infection. Cells were allowed to grow for 24 h. Cell extracts and supernatants and were harvested and assayed for the virus in cell extracts (a to d) and supernatants (e to h).

In the studies reported here, we showed that lipo-Tkip and lipo-SOCS1-KIR protected C57BL/6 mice against a highly lethal dose (2×10^6 PFU) of vaccinia virus. The i.p. injection of mimetics before and at the time of intranasal challenge with virus resulted in complete protection of mice at 100 and 200 μg of lipo-Tkip, 80% protection at 50 μg, and 20% protection at 10 μg. With lipo-SOCS1-KIR, we saw complete protection at 100 μg, 60% protection at 50 μg, and 20% protection at 10 μg. Alanine substitutions for phenylalanine at positions 56 and 59 of KIR and residues 8 and 11 of Tkip resulted in loss of protection. These residues in the KIR of SOCS-1 have previously been identified as crucial to SOCS-1 function (36). Postinfection treatment with 200 μg Tkip or SOCS1-KIR starting 1 day after a challenge resulted in 80% protection, while day 2 postinfection treatment resulted in 20 to 40% protection. By comparison, the ErbB-1 inhibitor CI-1033 did not possess any postinfection therapeutic protection (35). Oral administration of 1,000 μg Tkip or SOCS1-KIR at days −2, −1, and 0 of a vaccinia virus challenge resulted in complete protection against the challenge, 500 μg resulted in 80% protection, and 250 μg provided 20% protection. Thus, Tkip and SOCS1-KIR were as effective as the other tyrosine kinase inhibitors in protecting mice against vaccinia virus under conditions where protected mice were subjected to a greater virus challenge load (28, 35). Further, the mimetics showed postinfection therapeutic efficacy, which was not demonstrated by the other kinase inhibitors.

The tyrosine kinase inhibitors Gleevec and CI-1033 did not affect virus replication and assembly but rather affected release from the cell membrane involving actin tails, thus limiting the ability to infect adjacent cells (28, 35). Multiple cellular kinases, including Src, Fyn, Yes, Abl, and Arg, have been shown to be involved in poxvirus release from infected cells, and Gleevec inhibits Abl (28). Poxvirus growth factors such as VGF for vaccinia virus and SPGF for variola virus act on the ErbB-1 receptor, which plays a role in the activation of c-Src, so one way that CI-1033 could inhibit vaccinia virus release is by inhibiting the activation of c-Src by ErbB-1 (35).

We have previously shown that SOCS-1 mimetics, like SOCS-1, inhibit ErbB-1 and JAK2 (13, 14, 33). Similarly, as indicated above, the increased phosphorylation of both ErbB-1 and JAK2 observed in early stages of infection with vaccinia virus was significantly inhibited by the mimetics. Decreased phosphorylation of JAK2 was also observed in myxoma virus-infected cells in the presence of the tyrosine kinase inhibitor tyrophostin AG490 (21). This inhibition was associated with a corresponding inhibition of virus replication.

Unlike Gleevec and CI-1033, the SOCS-1 mimetics inhibited vaccinia virus replication in cells, since both the intracellular and extracellular virus levels were significantly reduced in one-step growth curve experiments compared to those of untreated or control peptide-treated cells. Early and possibly later transcription, as assessed by the corresponding inhibition of gene expression of the D12L, A1L, and A7L proteins by SOCS1-KIR and Tkip, suggests that the SOCS-1 mimetics had an inhibitory effect on all stages of vaccinia virus growth. This was confirmed by the inhibition of replication even when mimetics were added to cells at 4 h postinfection, where late gene expression was shown. The ability to inhibit JAK2 was probably key to the inhibition of virus replication over a broad time range, as tyrophostin AG490, an inhibitor of JAK2 and other tyrosine kinases, had a similar inhibitory effect on myxoma virus replication (21). It is significant that alanine substitution-containing mimetics did not affect virus replication, consistent with a lack of protection of vaccinia virus-infected mice. The ability of the mimetics to inhibit virus replication may explain why they are better postinfection therapeutics in vaccinia virus infection than the other tyrosine kinase inhibitors, which inhibit release but not replication of virus. The mimetics

also probably have a broader kinase-inhibitory function, since they inhibit JAKs and ErbB-1. Additionally, we have shown that, like SOCS-1, the mimetics inhibit lipopolysaccharide activation of TLR4, probably at the stage of Btk phosphorylation of Mal (37; unpublished data). SOCS-1 mimetics are thus effective inhibitors of vaccinia virus replication in induction of their antiviral activity.

Tkip was the first SOCS mimetic that we developed, and its development, unlike that of SOCS1-KIR, was based on hydropathic complementarity to the activation loop of JAK2 (13). Thus, there was no consideration of homology to any domain or region of any of the SOCS proteins. Only SOCS-1 and SOCS-3 were thought to possess a KIR (4). Recently, a putative KIR of SOCS-5 has been identified, buttressed by a striking similarity to the amino acid sequence of Tkip (11). Thus, the empirical development of a SOCS mimetic has helped identify a KIR of SOCS-5. This observation suggests that development of SOCS mimetics such as Tkip provided insight into the identification of functional sites in SOCS, as well as the application of such findings in the development of novel antivirals. These findings are of particular interest as both Tkip and SOCS-5 are potent inhibitors of the EGF receptor (data above) (25), an important player in poxvirus replication (9, 10, 26, 35).

The use of SOCS-1 mimetics in the treatment of viral diseases such as those caused by poxviruses reveals an endogenous regulatory system that previously was not known to have an antiviral function. This endogenous antipoxvirus system apparently does not depend on IFN. In fact, it inhibits JAKs that are involved in IFN signaling. These JAKs and other tyrosine kinases such as ErbB-1 are thus apparently indispensable to poxvirus replication. SOCS mimetics may therefore be applicable to other intracellular pathogens, such as bacteria and parasites, that make use of growth factors of pathogen or host origin for their virulence where tyrosine kinases play a critical role.

ACKNOWLEDGMENTS

This work was supported by NIH grants R01 AI 056152 and R01 NS 051245 to H.M.J. L.L.H. was partly supported by NSF grant DBI-0649198.

We thank S. M. I. Haider for peptide synthesis.

REFERENCES

1. **Ahmed, C. M., M. A. Burkhart, M. G. Mujtaba, and H. M. Johnson.** 2005. Peptide mimetics of gamma interferon possess antiviral properties against vaccinia and other viruses in the presence of poxvirus B8R protein. J. Virol. **79:**5632–5639.
2. **Ahmed, C. M. I., and H. M. Johnson.** 2006. IFN-γ and its receptor subunit IFNGR1 are recruited to the IFN-γ-activated sequence element at the promoter site of IFN-γ-activated genes: evidence of transactivational activity in IFNGR1. J. Immunol. **177:**315–321.
3. **Ahmed, C. M., J. P. Martin, and H. M. Johnson.** 2007. IFN mimetic as a therapeutic for lethal vaccinia virus infection: possible effects on innate and adaptive immune responses. J. Immunol. **178:**4576–4583.
4. **Alexander, W. S., and D. J. Hilton.** 2004. The role of suppressors of cytokine signaling (SOCS) proteins in regulation of immune response. Annu. Rev. Immunol. **22:**503–529.
5. **Ausubel, F. M., R. Brent, R. E. Kingston, D. D. Moore, J. G. Seidman, A. Smith, and K. Struhl (ed.).** 2002. Short protocols in molecular biology, p. 16–65. Wiley, New York, NY.
6. **Baker, R. O., M. Bray, and J. W. Huggins.** 2003. Potential antiviral therapeutics for smallpox, monkeypox and other orthopox virus infections. Antivir. Res. **57:**13–23.
7. **Barry, M., and G. McFadden.** 1997. Virus encoded cytokines and cytokine receptors. Parasitology **115:**S89–S100.
8. **Bazer, F. W., T. E. Spencer, and T. L. Ott.** 1996. Placental interferons. Am. J. Reprod. Immunol. **35:**297–308.
9. **Buller, R. M. L., S. Chakrabarti, J. A. Cooper, D. R. Twardzik, and B. Moss.** 1988. Deletion of the vaccinia virus growth factor gene reduces virus virulence. J. Virol. **62:**866–874.
10. **Buller, R. M., S. Chakrabarti, B. Moss, and T. Fredrickson.** 1988. Cell proliferative response to vaccinia virus is mediated by VGF. Virology **164:**182–192.
11. **Croker, B. A., H. Kiu, and S. E. Nicholson.** 2008. SOCS regulation of the JAK/STAT signaling pathway. Semin. Cell Dev. Biol. **19:**414–422.
12. **De Clercq, E.** 2001. Vaccinia virus inhibitors as a paradigm for the chemotherapy of poxvirus infections. Clin. Microbiol. Rev. **14:**382–397.
13. **Flowers, L. O., H. M. Johnson, M. G. Mujtaba, M. R. Ellis, S. M. Haider, and P. S. Subramaniam.** 2004. Characterization of a peptide inhibitor of Janus kinase 2 that mimics suppressor of cytokine signaling 1 function. J. Immunol. **172:**7510–7518.
14. **Flowers, L. O., P. S. Subramaniam, and H. M. Johnson.** 2005. A SOCS-1 peptide mimetic inhibits both constitutive and IL-6 induced activation of STAT3 in prostate cancer cells. Oncogene **24:**2114–2120.
15. **Harrop, R., M. G. Ryan, H. Golding, I. Redchenko, and M. W. Carroll.** 2004. Monitoring of human immunological responses to vaccinia virus, p. 243–265. *In* S. N. Isaacs (ed.), Vaccinia virus and poxvirology. Humana Press, Totowa, NJ.
16. **Jahrling, P. B., E. A. Fritz, and L. E. Hensley.** 2005. Countermeasures to the bioterrorist threat of smallpox. Curr. Mol. Med. **5:**817–826.
17. **Kim, M., H. Yang, S. K. Kim, P. A. Reche, R. S. Tirabassi, R. E. Hussey, Y. Chishti, J. G. Rheinwald, T. J. Morehead, T. Zech, I. K. Damon, R. M. Welsh, and E. L. Reinherz.** 2004. Biochemical and functional analysis of smallpox growth factor (SPGF) and anti-SPGF monoclonal antibodies. J. Biol. Chem. **279:**25838–25848.
18. **Kyte, J., and R. F. Doolittle.** 1982. A simple method for displaying the hydropathic character of a protein. J. Mol. Biol. **157:**105–132.
19. **Leaman, D. W., S. Leung, X. Li, and G. R. Stark.** 1996. Regulation of STAT-dependent pathways by growth factors and cytokines. FASEB J. **10:**1578–1588.
20. **Leung, S., S. A. Qureshi, I. M. Kerr, J. E. Darnell, Jr., and G. R. Stark.** 1995. Role of STAT2 in the alpha interferon signaling pathway. Mol. Cell. Biol. **15:**1312–1317.
21. **Masters, J., A. A. Hinek, S. Uddin, L. C. Platanias, W. Zeng, G. McFadden, and E. N. Fish.** 2001. Poxvirus infection rapidly activates tyrosine kinase signal transduction. J. Biol. Chem. **276:**48371–48375.
22. **McFadden, G.** 2005. Poxvirus tropism. Nat. Rev. Microbiol. **3:**201–213.
23. **Moss, B., and J. L. Shisler.** 2001. Immunology 101 at poxvirus U: immune evasion genes. Semin. Immunol. **13:**59–66.
24. **Myskiw, C., Y. Deschambault, K. Jeffries, R. He, and J. Cao.** 2007. Aurintricarboxylic acid inhibits the early stage of vaccinia virus replication by targeting both cellular and viral factors. J. Virol. **81:**3027–3032.
25. **Nicholson, S. E., D. Metcalf, N. S. Sprigg, R. Columbus, F. Walker, A. Silva, D. Cary, T. A. Wilson, J. Zhang, D. J. Hilton, W. A. Alexander, and N. A. Nicola.** 2005. Suppressor of cytokine signaling (SOCS)-5 is a potential regulator of epidermal growth factor signaling. Proc. Natl. Acad. Sci. USA **102:**2328–2333.
26. **Opgenorth, A., D. Strayer, C. Upton, and G. McFadden.** 1992. Deletion of the growth factor gene related to EGF and TGF-α reduces virulence of malignant rabbit fibroma virus. Virology **186:**175–191.
27. **Prichard, M. N., and E. R. Kern.** 2005. Orthopoxvirus targets for the development of antiviral therapies. Curr. Drug Targets Infect. Disord. **5:**17–28.
28. **Reeves, P. M., B. Bommarius, S. Lebeis, S. McNulty, J. Christensen, A. Swimm, A. Chahroudi, R. Chavan, M. B. Feinberg, D. Veach, W. Bornmann, M. Sherman, M., and D. Kalman.** 2005. Disabling poxvirus pathogenesis by inhibition of Abl-family tyrosine kinases. Nat. Med. **11:**731–739.
29. **Sliva, K., and B. Schnierle.** 2007. From actually toxic to highly specific novel drugs against poxviruses. Virol. J. **4:**8.
30. **Stanford, M. M., G. McFadden, G. Karupiah, and G. Chaudhri.** 2007. immunopathogenesis of poxvirus infections: forecasting the impending storm. Immunol. Cell Biol. **85:**93–102.
31. **Szente, B. E., J. M. Soos, and H. M. Johnson.** 1994. The C-terminus of IFN-γ is sufficient for intracellular function. Biochem. Biophys. Res. Commun. **203:**1645–1654.
32. **Tzahar, E., J. D. Moyer, H. Waterman, E. G. Barbacci, J. Bao, G. Levkowitz, M. Shelly, S. Strano, R. Pinkas-Kramarski, J. H. Pierce, G. C. Andrews, and Y. Yarden.** 1998. Pathogenic poxviruses reveal viral strategies to exploit ErbB signaling network. EMBO J. **17:**5948–5963.
33. **Waiboci, L. W., C. M. Ahmed, M. G. Mujtaba, L. O. Flowers, J. P. Martin. M. I. Haider, and H. M. Johnson.** 2007. Both the suppressor of cytokine signaling (SOCS-1) kinase inhibitory region and SOCS-1 mimetic bind to JAK2 autophosphorylation site: implications for the development of a SOCS-1 antagonist. J. Immunol. **178:**5058–5068.
34. **Yang, G., D. C. Pevear, M. H. Davies, M. S. Collett, T. Bailey, S. Rippen, L. Barone, C. Burns, G. Rhodes, S. Tohan, J. W. Higgins, R. O. Baker, R. L. M. Buller, E. Touchette, K. Waller, J. Schriewer, J. Neyts, E. DeClercq, K. Jones, D. Hruby, and R. Jordan.** 2005. An orally bioavailable antipoxvirus

compound (ST-246) inhibits extracellular virus formation and protects mice from lethal orthopoxvirus challenge. J. Virol. **79:**13139–13149.
35. **Yang, H., K. Sung-Kwon, M. Kim, P. A. Reche, T. J. Morehead, I. K. Damon, R. M. Welsh, and E. L. Reinherz.** 2005. Antiviral chemotherapy facilitates control of poxvirus infections through inhibition of cellular signal transduction. J. Clin. Investig. **115:**379–387.
36. **Yasukawa, H., H. Misawa, H. Sakamoto, M. Masuhara, A. Sasaki, T. Wakioka, S. Ohtsuka, T. Imaizumi, T. Matsuda, J. N. Ihle, and A. Yoshimura.** 1999. The JAK-binding protein JAB inhibits Janus tyrosine kinase activity through binding in the activation loop. EMBO J. **18:**1309–1320.
37. **Yoshimura, A., T. Naka, and M. Kubo.** 2007. SOCS proteins, cytokine signalling and immune regulation. Nat. Rev. Immunol. **7:**454–465.